

Grip Force and Slip Analysis in Robotic Grasp: New Stochastic Paradigm Through Sensor Data Fusion

Debanik Roy
Bhabha Atomic Research Centre
India

1. Introduction

Algorithmic *data fusion* is instrumental in evaluating the quantitative output of a multi-sensory system and the same becomes extremely challenging, especially when the elemental sensory units do vary in type, size and characteristics. Truly, fusion of such *heterogeneous* sensory data remains an open-research paradigm till date, especially in the field of robotics, owing to its inherent characteristics in quantifying the output response of the system. The problem gets even critical when we need to contour with a limited number of elemental sensor-cells (*taxels*), in contrast to traditional theories dealing with large agglomeration of (identical) sensor units. In fact, fusion models used hitherto have been found to be largely inappropriate for the distinct object-groups, e.g. from point-mass to small-sized ones. Besides, paradigms of grasp synthesis (grip force & slippage) were largely unattended. Although traditional theories on sensory data fusion fit quite satisfactorily in searching a pre-defined object with a tentative dimension and depth perception, they fail to do justice in cases where profile of the object do vary from micro-scale to a finite spatial dimension. In answering these lacunas, the present article dwells on modeling, algorithm and experimental analysis of three novel fusion rule-bases, which are implemented in small-sized tactile array sensor to be used in robot gripper. A new proposition has been developed for assessing the *decision threshold*, signaling the *presence of object* inside the grasp-zone of the gripper. Besides, the developed model evaluates the approximate planar area of the grasped object alongwith its shape in real-time. The model also provides estimate for the gripping force required to sustain a stable grasp of the object vis-à-vis slippage characteristics, if any. Signal detection with multiple sensors, either all similar or dissimilar or any arbitrary combination, can be performed in two manners. In the traditional method, the local sensors communicate all *observations* (raw data) directly to a *centralized detector* (e.g. system controller board) where decision processing is performed. This method, although incorporates parallel channels for data communication, often requires a large bandwidth for the communication channels in order to obtain real-time results. In contrary, the second method deals with each sensor individually, by associating a *detector* module to each of the sensor-cells, which *decides locally* whether a signal is detected or not. These *local decisions* get transmitted to the main controller unit (traditionally called "Data Fusion Center" in the literature), where those get *unified* for *global* decision. Although this method suffers from

Open Access Database www.intechweb.org

Source: Sensors, Focus on Tactile, Force and Stress Sensors, Book edited by: Jose Gerardo Rocha and Senentxu Lanceros-Mendez, ISBN 978-953-7619-31-2, pp. 444, December 2008, I-Tech, Vienna, Austria

loss of information, yet it is the most optimal choice for sensory system design because of high reliability, compact hardware, lower cost and a user-friendly operative environment. In fact, this group of signal processing via localized decision vis-à-vis the field of 'Decentralized / Distributed Decision Making' has been an active area of research, wherein the realization has come out in the manner that these very problems are qualitatively different from the corresponding decision thematic with centralized information. It is, perhaps, wise to conjecture that the prohibitive factor in decentralized problems is not so much the inadequacy of the mathematical tools presently been used, rather the inherent complexity of the problems that have usually been formulated.

The classical theory of optimal sensor signal processing is based on 'Decentralized Testing & Augmentation', using statistical estimation and hypothesis testing methods. The logically driven coherent *unified* output of the said aggregation is being used for processing allied control system signals of the robotic / gripper system. Unlike most of the decentralized control problems, the hypothesis-testing problem can be solved in a relatively straightforward way. This is due principally to the fact that since the decisions made do not get looped back into the system dynamics, those do not affect the information of other decision makers either. However, even in the case of independent observations, several types of unusual behaviour can occur. For example, the threshold computations can yield locally optimal thresholds, which are far from the globally optimal values. The paradigm of decentralized sensor fusion has hitherto been attributed largely by Bayesian Theory, which deals quite robustly the situations involving probabilistic hypothesis testing but fails to address the cases where fuzziness is involved in the main process itself. On the contrary, Dempster-Shafer Theory tackles only those problems where system caters for fuzzy concepts. Unfortunately both of the theories are inadequate so far as the data fusion in mechatronic system is concerned.

We propose a new fusion theory wherein the threshold for fusion can be suitably adapted depending upon the end-application. The proposed schemata provides insight to two aspects, namely evolution of new rule-bases towards data fusion and an optimized inference about object's presence or absence based on stochastic hypothesis testing model. This *dynamic thresholding* of the proposed hypothesis helps fusing the sensory data from the physical device (a multi-input heterogeneous tactile array sensor in the present case), based on the requirement of the user. Moreover, the *fusion rules*, do represent a unique strategy for assimilating the *raw* sensor data. The threshold estimation has been based on using the *variable limits*, exploiting the metrics of Type I error (i.e. rejecting the Alternative Hypothesis when true), as well as Type II error (i.e., accepting the Null Hypothesis when false), corresponding to three different fusion rule-bases. The aim of our work in developing a tailor-made fusion-based hypothesis is concentrated on two vital aspects, viz. it should be able to i] *cater large number of sensor-cells*, which are heterogeneous in nature and ii] *sense the presence of tiny 'point-objects'* on the gripper surface. It may be mentioned that both of these two paradigms were overlooked in the researches hitherto and thus, the existing fusion cum hypothesis testing models are unsuitable to real-life applications in robotics. In the contrary, our model of data fusion and statistical hypothesis testing with new threshold thematic will ensure reliable measure towards overall *quantization* (e.g. overall external shape, surface area and approximate contour) of the object(s) present in the vicinity of the gripper. In our model, hypotheses are postulated corresponding to different types of sensory outputs. Here, we will differ from the traditional nomenclatures for Null Hypothesis (H_0) as "Signal is

absent" against Alternative Hypothesis (H_1) as "Signal is present", in order to suit our requirement towards robotic grasp-based situations. We, therefore, define the hypotheses as *Significant Object Present* [SOP] vs. *Significant Object Absent* [SOA] respectively for ' H_1 ' and ' H_0 '. We define "Significant Object" as those objects whose surface area is larger than that of the graspable area of the gripper or in other words, larger than the sensing area of the gripper. We prefer to adhere to the bi-modal hypothesis paradigm and represent the inherent *fuzziness* in decision-making process with *white noise*, having a relatively higher value of Signal-to-Noise Ratio (SNR). Three novel *Fusion Rule-bases*, viz. [a] *Multiplicative*, [b] *Additive* and [c] *Preferential Selection*, have been formulated in order to reveal the inter-cell relationship of the array (matrix) sensor. In other words, these rule-bases are devised to represent the exact way the elemental cells (*taxels*) are 'reacting' with one another. We will finally have a logical *unified* output from the system controller using these rule-bases and individual signal-output from the taxels. The *dynamic (global) threshold*, as proposed in our model, is to be selected optimally using the user-specified value of either probability of Type I error or Type II error. The filtered sensory data is used to estimate the optimal value of the grip force, which is required to be applied by the jaw to maintain stable vis-à-vis slip-free firm grasp. Nonetheless, the developed model will also ensure the user regarding the characteristics of the post-grasp slip, if any.

Although traditional surveillance problem with multiple sensors and optimization therein using log-likelihood function have been addressed substantially in last two decades (Chair & Varshney, 1986) & (Gustavo & Grajal, 2006), it lacks generality in situations of sensing 'point-objects'. These algorithms are based on an approach wherein maximum likelihood of remotely located unknown signal(s) can be estimated under white Gaussian noise, but the techniques can't be adopted for sensing *localized* sensor-signals.

Field-sensor outputs in a distributed tracking vis-à-vis surveillance system are categorized in two broad groups, depending on a) the *modus operandi* or activation syntax (parallel or serial) and b) the physical layout (staggered or synchronous). Unlike the case of distributed decision making in parallel, fusion problem with the configurations of sensors in serial chain (Viswanathan et al, 1988), (Hashemi & Rhodes, 1989) & (Swaszek, 1993) may have better performance over the parallel distribution case for two sensors. However, the methods perform poorly for large sensor-cells, which is the typical case in real-life applications. Likewise, a comparative study on the system performance was made using temporally staggered sensors as well as synchronous sensors, using a novel metric, namely, average estimation error variance (Niu et al, 2005). Irrespective of the *modus operandi*, serial or parallel, selection of *local node* in a distributed sensor network is crucial, as it will govern the decision-making system regarding the incorporation of the corresponding data for surveillance (Kaplan, 2006).

Tracking of remote target using multiple field-sensors is a well-researched field, irrespective of its genesis; vide *static target* [e.g. a rigid sensor rig] (Chroust & Vincze, 2004) or *maneuvering target* (Jeong & Tugnait, 2005). In case of static targets, e.g. presence of objects in the vicinity of the gripper-sensor, an estimation of the bias in outputs of the asynchronous field-sensors is important. The decoupling between the numerical estimations for the target state and the sensor bias is attained, considering, a) the cross-covariance between the state & bias estimates (Lin et al, 2005) and b) the reduced bias estimate of the joint probabilistic data association (JPDA) algorithm (Kalandros & Pao, 2005). However, for large number of sensor-cells, like the case of ours, the performance of the distributed tracker has been found

degrading in comparison to centralized estimation, despite using optimal track-to-track fusion algorithm (Chen et al, 2003).

In contrast to log-likelihood method, the fusion tests to be adopted for achieving maximized probability of detection (for a fixed probability of false alarm) should ideally be Neyman – Pearson [N-P] (Srinivasan, 1986). Nonetheless, the threshold of N-P test becomes data dependent if the conditional impedance is removed (i.e. hypotheses are not truly statistically independent) and does not yield any easy solution for optimization (Tsitsiklis & Athans, 1985). Moreover, N-P fusion rule needs the sensor error probabilities (i.e. probability of false alarm & probability of miss) to be known a-priori and those must not be altered during the fusion process. These are very stringent precludes to the decision paradigms that degrade the performance of the data fusion (El-Ayadi, 2002).

The solution of data fusion problem for fixed binary local detectors with statistically independent decisions (Chair & Varshney, 1986) was amplified and extended for i] correlated local binary decisions (Moshe, 1992) and ii] team hypothesis testing and environmental simulation (Tenney & Sandell, 1981a), (Sadjadi, 1986), (Reibman, 1987), (Papastavrou & Athans, 1992) or iii] multidimensional data association (Kirubarajan et al, 2001), (Gan & Harris, 2001); iv] covariance control (Kalandros & Pao, 2002) and v] new design for low-bandwidth track fusion (Ruan & Willett, 2005). In fact, the fused decision in a distributed data fusion problem for similar as well as dissimilar sensors using N-P test is transmitted alongwith a quality information in numerical terms, viz. 'degree of confidence' (Thomopoulos et al, 1987). Various methodologies, such as *extended Kalman filter* (Nabaa & Bishop, 1999), *layered neural networks* (Karniely & Siegelmann, 2000) or *Bayesian estimation* (Okello & Challa, 2004) have been postulated towards fixing sensor alignment problems (known as sensor registration in the literature) in distributed fusion, unlike the method of maximum likelihood estimator, used hitherto.

Another school of thought in fusion optimization is using time-varying global threshold, which essentially calls for the solution of two coupled sets of dynamic programming equations for computation (Tenney & Sandell, 1981b,c), (Teneketzis & Varaiya, 1984) & (Tang, 1991). The case of decentralized detection system with feedback and memory using the Bayesian formulation is investigated (Alhakum & Varshney, 1996), wherein the optimization gets summed up in a likelihood ratio test at the local detectors for statistically independent observations. However, the process gets computationally intensive once the system has a large number of sensors (Moshe et al, 1991). Although the universality of Bayesian approach is recognized for computational transparency (Moshe et al, 1999), yet a few specific situations are better analyzed either through Dempster - Shafer theory (Murphy, 1998) or another novel theory (Thomopoulos, 1990), which gives a good trade-off between the Bayesian and D-S approaches. Interestingly, the inherent uncertainty in a two-hypothesis model is also alleviated in a recent research, by considering a discrete decision zone between Null & Alternate Hypothesis (Wang, 1998). However, irrespective of the major three techniques used in hypothesis testing, e.g. Log-likelihood Ratio [LLR], N-P or D-S, one lacuna is surfacing that the potential of Type I and Type II error shielding is not utilized to a proper extent. But these two cut-offs, i.e. Type I & Type II error can be of significant relevance in defining global thresholds and to be specific, this potential has been used in our architecture. Our methodology essentially involves a *non-parametric stochastic adaptive decision fusion*, wherein fusion center knows only the number of the sensors under each sub-types, but does not consider their error probabilities. In contrast to non-stochastic

fusion algorithms, e.g. (El-Ayadi, 2002), our technique uses a hypothesis error-based global threshold for the final decision regarding the *target* (i.e. presence of object near the graspable zone of the robot gripper).

The first two rule-bases and the developed hypothesis, described here, have been tested with an indigenous tactile array-sensor, comprising three types of taxels, namely, resistive cells (*R-cells*), capacitive cells (*C-cells*) and piezo cells (*P-cells*) placed in matrix. The sensor has got 61 elemental taxels in total, each of which provides calibrated output (in mV) when excited with external forcing. However, we will consider the readings from 57 taxels, which will be sufficient for experimental investigation. Out of these 57 taxels, 32 taxels belong to R-cells, while C-cells & P-cells constitute 21 & 4 taxels respectively. The sensor has been simulated for two-jaw grasp (i.e. considering it as a gripper-sensor) and experimented with a variety of objects impinging over it. The sensory output is processed for the determination of object's presence alongwith its size & shape and used for the evaluation of grip as well as slip force. On the other hand, the *Preferential Selection* rule-base was tested through a two-jaw sensor-instrumented robotic gripper, having 18 heterogenous taxels in total, distributed in three categories, viz. load cells (*L-cells*), thin-beam sensors (*TBS-cells*) & infrared sensors (*IR-cells*), bearing 2, 10 & 6 taxels respectively.

2. Hypothesis testing and proposed schemes of data fusion

2.1 Formulation of statistical hypothesis

We prefer to adhere to the bi-modal hypothesis paradigm and represent the inherent *fuzziness* in decision-making process with *white noise*, having a relatively higher value of Signal- to -Noise Ratio (SNR). Nonetheless, these two hypotheses have been re-modeled from real-life perspective as shown below,

$$H_0: X_i = N_i \tag{1}$$

$$H_1: X_i = S + N_i, \quad \forall i = 1, 2, 3, \dots, n$$

where, X_i : Observation vector of the i^{th} sensor; N_i : Noise vector at the i^{th} sensor; S: Actual detectable signal vector; n: Total number of sensors in the system. The a-priori probabilities of ' H_0 ' and ' H_1 ' are: $P(H_0) = P_0$ and $P(H_1) = P_1$. We assume all of these ' i ' detectors ($\forall i=1, 2, \dots, 57$ in case of matrix sensor & $i=1, 2, \dots, 18$ for jaw-gripper) have observations at the individual detector level, denoted by, X_i . Now, each detector employs a "Decision Rule", in order to make a decision-vector ' u_i ', which is the *localized* logistic metric. Let, logistic parameter, $\{u_i\}$, $\forall i=1, 2, \dots, 57$ or 18, be defined against individual sensor-cells, such that, $u_i = -1$, if H_0 is true and $= +1$, if H_1 is true. We also consider the activation syntax of the data fusion to follow *serial* path. Nonetheless, the set $\{u_i = +1\}$ is to be arrived at by considering a cut-off value, ζ , in the following manner,

$$\{u_i = +1\} = \{\forall u_i, i \in u_{s^+}\} \tag{2}$$

where, u_{s^+} is mapped as,

$$u_{s^+} \xrightarrow{\text{mapping}} (X_i - N_i) \geq \zeta \tag{3}$$

and,

$$[X_i] - [N_i] = [Y_i] \tag{4}$$

We further assume that the observations at the individual detectors are statistically independent and the conditional probability density function is described by, $P(Y_i / H_k)$, $\forall i=1,2,\dots,57$ or 18 & $\forall k=0,1$. The stated propositions are equally valid for $\{u_i\} = [0,1]$ tuple $\forall i=1,2,\dots,n$, wherein "0" signifies truth of H_0 and "+1" is correlated to occurrence of H_1 . Nonetheless, the Global U , viz. ' U_G ' will be a function of all the elemental fused data, i.e., ' u_i '. In other words, it essentially means that the global fused data, $\{U_G\}$, is an extrinsic function of $\{u_i\}$, i.e. $\{U_G\} = f(u_1, u_2, \dots, u_N)$, where $N=57$ or 18 , depending upon the total number of taxels. The proposed method of inference relies on a 'variable limit' or *dynamic threshold*, which is to be estimated through a mathematical model. The location of the dynamic threshold limit is dependent on the confidence level for rejecting ' H_1 ', chosen a-priori, i.e. on the numerical value of Type I or Type II error.

2.2 Development of fusion rules

2.2.1 "k-out-of-n" logic revisited

Before detailing out the proposed application-oriented fusion rules, we would examine the "k-out-of-n" logic, used hitherto as a quick reference to the evaluation of fusion hypothesis. The rule verdicts "presence of object" if 'k' or more detectors select ' H_1 ' at the elemental detection level out of total 'n' detectors. As a matter of fact, considering the set of ' u_i ' as $\{u_i\}=[-1,1]$, for first two rule-bases, U_G is syntaxed as,

$$U_G = +1, \text{ if } (u_1 + u_2 + \dots + u_{57}) \geq 2k - n$$

$$= -1, \text{ otherwise.}$$

Although the rule clearly demarcates the acceptance or rejection of ' H_1 ' in case of large objects (i.e. objects having planar area sufficiently more than that of the sensing area), it fails to demarcate adequately the occurrence of 'point-force', unless we define $k=1$ a-priori. It may be stated that barring its marginal limitations, this logic has been imbibed by most of the decentralized fusion metric, by and large. However, the bottleneck in fusion problem with "k-out-of-n" logic can be tackled more elegantly using the concept of threshold, as used in Bayesian estimation theory. Our rules will hence follow the *Global Thresholding* principle in evaluating the test hypotheses. However, in contrast to "k-out-of-n" logic, the new rules will propose acceptance or rejection of ' H_1 ' on the basis of numerical value of U_G and the value of *dynamic threshold* considered in that situation. By definition, it is the global threshold only, but we call it *dynamic* as its value gets changed depending upon the application environment. This dynamic threshold can be evaluated numerically from the system parameters, known a-priori. Thus, in true sense, the new rules are functionally in inverse proposition with respect to "k-out-of-n" logic.

2.2.2 Syntax of the fusion rules developed

The first two novel *Fusion Rule-bases*, viz. *Multiplicative* and *Additive*, have been formulated in order to reveal the inter-cell relationship of the matrix sensor, while the third one, i.e. *Preferential Selection*, is aimed at revealing the inter-cell relationship of the semi-matrix layout of the jaw gripper sensors. In other words, these rule-bases have been devised to represent the exact way the taxels are 'reacting' with one another, i.e. in what way these taxels are 'influencing' the neighbouring taxels and/or getting influenced by those. We will finally have a logical *unified* output from the system controller, considering the set of ' u_i ' as

$\{u_i\}=[-1,1]$. All the three rule-bases culminate in a non-zero value of U_G for $\{u_i\}=[-1,1]$ and the evaluation is *unbiased* so far as the object-size is concerned. The Multiplicative model defines ' U_G ' as,

$$U_G = \prod_{i=1}^{i=n} e^{u_i} = (e)^{n-2k} \tag{5}$$

while, the Additive model postulates the definition of ' U_G ' as,

$$U_G = \sum_{i=1}^{i=n} u_i = (n - 2k) \tag{6}$$

where, $\{u_i\}$: localized decision for the i^{th} . taxel, $\forall i =1,2,\dots,n$; ' n ': total number of taxels activated in the sensor and ' k ': number of taxels giving output as "-1", i.e. "signal absent". Now, the *fused* decision regarding the selection of test hypothesis will be ruled by the evaluation paradigm, decided a-priori. In our model, we use the numerical value of the *dynamic threshold* ($\lambda_{Threshold}$) as the evaluation metric. We define the evaluation metric for both of the models as: if $U_G \geq \lambda_{Threshold}$, then accept H_1 , otherwise reject H_1 . In a similar manner, we can obtain the values of U_G using $\{u_i\}=[0,1]$ tuple for multiplicative and additive models also. For multiplicative model, the value of U_G will be e^{n-k} and for additive model the value of U_G will be equal to $(n-k)$.

Now, we define ' U_G ' under Preferential Selection model as,

$$U_G = \sum_{i=1}^{i=n} u_i (1 + u_{i+1})^p (1 + u_{i-1})^q \tag{7}$$

where, $\{u_i\}$: localized decision for the i^{th} . taxel, $\forall i =1,2,\dots,n$; ' n ': total number of taxels activated in the gripper sensor system; p : relative weightage of the succeeding taxel, i.e. $(i+1)^{th}$. cell and q : relative weightage of the preceding taxel, i.e. $(i-1)^{th}$. cell, where $0 \leq p, q \leq 2$. Exact numerical values of p & q need to be ascertained from experimentation with the sensory modules of the jaw-gripper. In that respect, eqn 7 is in a generalized format, which can be adapted for other similar systems as well. We also assume that in eqn. 7, $\{u_{i-1}\}_{i=1} = 0$ and $\{u_{i+1}\}_{i=n} = 0$. It may be noted that this model is essentially taxel-specific, unlike the previous models (vide eqn. 5& 6), wherein cumulative effect of the taxels are reflected only. In contrast, the *relative dependency* of one taxel over the neighbouring ones is getting priority in the present model. Hence, we have christened this model as '*preferential selection*', as the effect of adjoining taxels can be taken into consideration towards computing U_G , depending upon their relative influence/ importance. It may be stated that, this model, by definition, is best suited for taxels arranged in a row or column-wise fashion, i.e. applied for *row /column matrix*. Also, taxels may or may not be equally likely; nonetheless, we are unsure about the outcome (-1 or +1) of a specific taxel in the *grid*. It may be mentioned additionally here that the effect of relative dependency of the taxels could also be considered by another *sister-model* of U_G , viz. $U_G = \sum u_i (1 - u_{i+1})^p (1 - u_{i-1})^q$, but it would have been rather difficult to be interpreted graphically. Now, so far as the evaluation is concerned, we use the *dynamic threshold band* and the numerical value of the *mean threshold* ($\lambda_{Th-mean}$) as the evaluation metric in this rule-base. We define the evaluation metric as: if $U_G \geq \lambda_{Th-mean}$, then accept H_1 , otherwise reject H_1 . But, alongwith discrete acceptance / rejection, we will also encounter

one *fuzzy-zone*, which will signify *in-decision* regarding the acceptance or rejection of H_1 . Numerically, this in-decision zone will be directly proportional to the width of the threshold-band. It may be noted from eqns. 5 & 6 that the value of 'k' carries significance so far as the relative implications of it on $P(H_1)$ is concerned. Figure 1 shows the schematic view of the variation of $P(H_1)$ with 'k'. The first plot we considered is a simple straight-line plot while the other two are exponential fits.

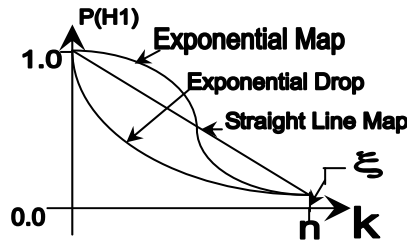


Fig. 1. Probability curves as per the fusion rules proposed

Based on the curves shown above, the mathematical formulae for evaluating $P(H_1)$ or in short, 'p' will be as follows,

$$p = \left(\frac{\xi - 1}{n}\right)(k) + 1 \quad \text{[For straight-line map]} \tag{8}$$

and,

$$p = \exp\left(\frac{\ln \xi}{n}\right)(k) \quad \text{[For exponential curves]} \tag{9}$$

2.2.3 HEBTEM: new strategy for selecting dynamic threshold

The *dynamic threshold*, as proposed in our model, is to be selected optimally using the user-specified value of either probability of Type I error or Type II error. It is termed as "Hypothesis Error Based Threshold Evaluation Method" (**HEBTEM**). The proposed method relies on the selection of the confidence level, as stipulated by probability of Type I or Type II error. However, we use probability of Type I error as the confidence level for additive model of fusion rule-base and probability of Type II error as the same for multiplicative model. For example, in case of multiplicative model of fusion, estimation using "2% non-confidence level" (i.e. probability of Type II error as 0.02) essentially declares the situation of 'object presence' with 98% certainty. We shall now investigate the situations in order to select the dynamic threshold using HEBTEM.

2.2.3.1 Using Multiplicative Model

Here, in-line with eqn. 9, an exponential curve has been fitted for the plot of $P(H_1)$ vs. U_G . The plot uses $\{u_i\} = [-1, +1]$ tuple and the generic representation of the *probability curve* is shown in fig. 2a. Similarly, we can get the plot of $P(H_1)$ vs. U_G for $\{u_i\} = [0,1]$ tuple too (refer fig. 2b). We assume that the probability of alternative hypothesis, i.e. $P(H_1)$ to be 0.5 when nearly half of the sensor-cells (i.e. 'n/2') will show "signal present", i.e. the value of 'k' becomes 'n/2' and that of U_G is 1.0. The final decision about "acceptance" and "rejection" of alternative hypothesis will be based on the location of global threshold (λ_{Th}) and the

observed value (represented as x' in fig. 2) of U_G . The scale along the X-axis of the plot also depicts the increment of U_G from e^{-n} to e^n , corresponding to the variation of ' k ', from n to 0 . We also assume that at $k = n$, i.e. when all the sensor-cells are giving $\{u_i\}=-1$, the occurrence of an object is *minimal*, which is quantified through ' ξ '. The numerical value of ' ξ ' is kept very small, in the order of 0.002 to 0.004, as found suitable for the matrix sensor. In fact, ' ξ ' is the true indication of the presence of 'point-mass' or 'point-force' over the gripper surface. Thus, we can identify two representative points in the plot, viz. (e^{-n}, ξ) and $(e^n, 1.0)$, which will be decisive in using the plot analytically.

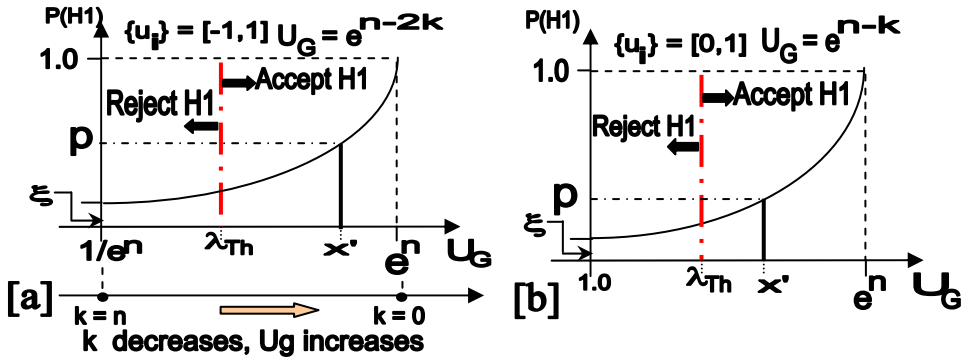


Fig. 2. HEBTEM with multiplicative model of data fusion for [a] $\{u_i\}=[-1,1]$ & [b] $u_i]=[0,1]$

As part of two-point interpolation for the exponential curve shown in fig. 2a, we consider the following transcendental equation involving ξ , viz.

$$P(H_1) \equiv p = a \exp^{mU_G} \tag{10}$$

It may be observed from the above equation that the value of both ' m ' and ' a ' can be evaluated numerically if ' ξ ' is known, vide,

$$m = \frac{e^n \ln \left(\frac{1}{\xi} \right)}{(e^{2n} - 1)} \tag{11a}$$

and

$$\ln \left(\frac{1}{a} \right) = \frac{e^{2n} \ln \left(\frac{1}{\xi} \right)}{(e^{2n} - 1)} \tag{11b}$$

2.2.3.2 Using additive model

Additive model of fusion rule-base considers probability of Type I error as the basis for ascertaining the presence or absence of object on the gripper. A graphical representation of the probability curve, using HEBTEM, is plotted in fig. 3 considering $\{u_i\}=[0,1]$ tuple. Considering an exponential fit for the probability distribution shown in fig. 3, the probability of alternative hypothesis becomes,

$$P(H_1) \equiv p = \xi \exp \frac{\ln\left(\frac{1}{\xi}\right) U_G}{n} \tag{12}$$

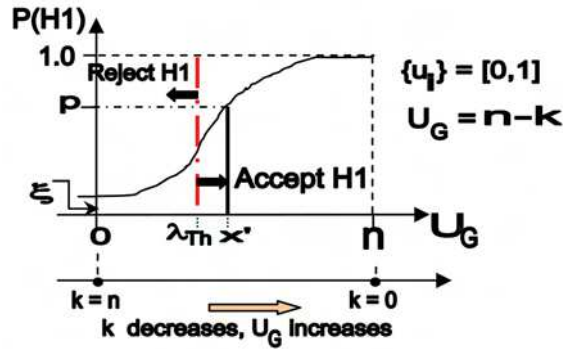


Fig. 3. Probability curve for additive model of fusion rule with $\{u_i\}=[0,1]$ using HEBTEM. However, paradigms of $P(H_1)$ plot changes significantly for $\{u_i\}=[-1,+1]$ tuple (refer fig. 4).

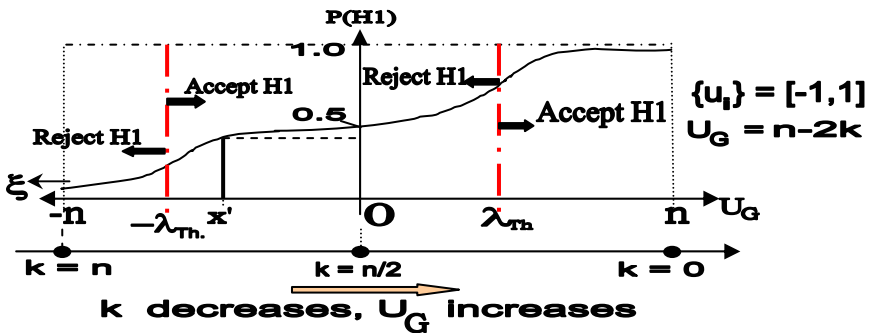


Fig. 4. Probability curve for additive model of fusion rule with $\{u_i\}=[-1,1]$ using HEBTEM

As articulated before, ξ symbolizes the presence of ‘point-mass’ or ‘point-force’ over the gripper surface. Here we can identify three representative points in the plot, viz. $(-n, \xi)$; $(0, 0.5)$ and $(n, 1.0)$, which will be used in formulating the transcendental equation involving ξ in order to evaluate $P(H_1)$. We will use a generic equation for the exponential curve, viz. $p = a \cdot e^{mx} + cx$, where ‘ p ’= $P(H_1)$; ‘ x ’= U_G and ‘ m ’ & ‘ c ’ are constant functions of ξ . The final equation, after three-point interpolation as stated above, becomes,

$$P(H_1) \equiv p = 0.5 \exp \frac{\ln\left\{\frac{(\xi+1)+\sqrt{\xi(\xi+2)}}{n}\right\} U_G}{n} + \left[\frac{1 - 0.5\{(\xi+1) + \sqrt{\xi(\xi+2)}\}}{n} \right] U_G \tag{13}$$

It is to be noted from eqn. 13 that we will use only positive values of ‘ m ’ and ‘ c ’, discarding the theoretically possible negative values of those. Also, unlike fig. 4, here we can use either of the two thresholds, namely ‘ λ_{Th} ’ or ‘ $-\lambda_{Th}$ ’, depending upon the application environment. In case we use a positive value for ‘ λ_{Th} ’, i.e. right-hand side of the curve, then the decision regarding the rejection /acceptance of ‘ H_1 ’ will be restricted to the right-hand-side zone of

the curve only. Likewise, if we intend to use the negative value for ‘ λ_{Th} ’, our decision has to be within the left-hand-side zone of the curve. Thus, in a way, additive model with $\{u_i\}=[-1,+1]$ tuple advocates *symmetric thresholding*, but not occurring simultaneously.

2.2.3.3 Using preferential selection model

A graphical representation of the probability curve for ‘ H_1 ’ as per this model is plotted in fig. 5 considering $\{u_i\}=[-1,1]$ tuple. Here we will characterize the threshold-band with three parameters, namely: ‘A’: $\lambda_{Th-initial}$; ‘B’: $\lambda_{Th-final}$ & the mid-point of the band as: $\lambda_{Th-mean}$.

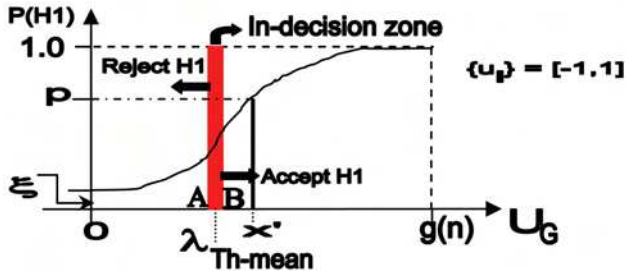


Fig. 5. Probability curve for the preferential selection model using HEBTEM

Using an exponential fit for the probability distribution shown in fig. 6, we have,

$$P(H_1) \equiv p = \left[\frac{1 - \xi}{\{g(n)\}^2} \right] U_G^2 + \xi \tag{14}$$

In eqn. 14, ξ symbolizes the presence of ‘point-mass’ or ‘point-force’ over the gripper surface and $g(n)$ signifies the gamut of the maximum possible values of U_G for various numerical combinations of (p,q) . The function $g(n)$ can be computed using the format of U_G , viz.

$$U_G = (2^p + 2^q) + (n - 2)[2^{(p+q)}], \quad \forall u_i = +1 \tag{15}$$

As per eqn 15, the values of $g(n)$, in ascending order will be, $\{g(n)\} : \{(2n-1), (4n-5), (4n-4), (8n-10), (16n-24)\dots\}$ for various combinations of (p,q) , where $\{p,q\} \subset [0,2]$. Figure 6 explains the geometric interpretation of $g(n)$, in evaluating U_G . Successive values of $g(n)$ are interpreted serially as $[g(n)]_1, [g(n)]_2, \dots, [g(n)]_k$, which becomes the yard-stick for the flattening of the probability curve, keeping ξ unaltered through-out.

2.2.3.4 Analysis of the Rule-bases and Evaluation of Dynamic Threshold

Major advantage of the proposed method, viz. HEBTEM, lies with the fact that it doesn’t include the concept of *Bayesian Risk*, which inherently involves the computation related to Probability of False Alarm (P_f) and Probability of Miss (P_m). The concept of *Bayesian Risk* is suitable only to cases where a large group of field-sensors are either attempting to evaluate the presence or absence of a single object or *tracking* a single *target*. In such a situation, all of the field-sensors do participate in the decision-making process and the output of each one of those will definitely be biased by its own $\{[P_f]-[P_m]\}$ tuple. But, in situations like robotic grasping or stand-alone tactile sensing, the use of sensor-cells will be governed by the actual size, shape and contour of the object to be ‘sensed’ and/or grasped.

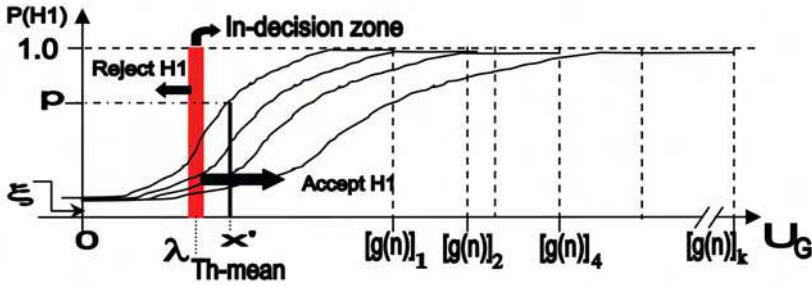


Fig. 6. Variation of probability curves under different tuples of the model

The value of the *dynamic threshold* (viz. λ_{Th} in figs. 2 to 4) can be estimated using either of the models, namely, multiplicative or additive. However, the paradigm of evaluation is different in these two cases. While multiplicative model of the fusion rule-base considers a non-confidence level (β), the additive model considers a confidence level (α), both chosen a-priori. It may be noted that the confidence level (α) for the additive model is nothing but the accepted level of probability of Type I error and ' β ' is the probability of Type II error. Figure 7 illustrates the philosophy of HEBTEM, wherein we have shown the zones of certainty and uncertainty for selecting 'H₁'. Here by ' $f(x)$ ' we mean the exponential curve for $P(H_1)$, vide eqns. 10, 12 & 13, i.e. corresponding to multiplicative & additive models using [-1,1] tuple.

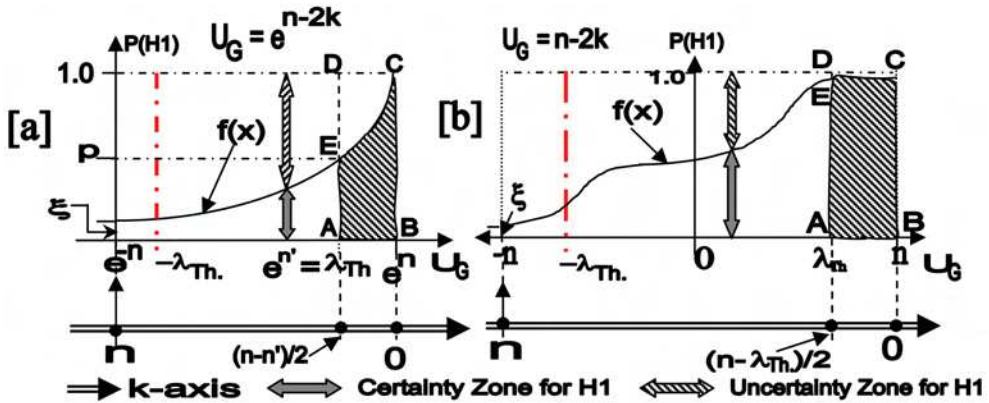


Fig. 7. Computation of dynamic threshold using [a] multiplicative & [b] additive model

It may be stated here that using an exponential fit for the multiplicative model is advantageous, because we can use a wider range of ' λ_{Th} ' with almost the same numerical value of ' β '. Thus in order to interpret the presence of *point-force /point-object*, it is wiser to consider such a ' λ_{Th} ', which is *closer* to the origin (i.e. the point with $k=n$). For these cases of point-force selection, the usual value of ' β ' will be quite large, because there will be a high tendency of selecting 'H₀' (refer the plots of fig. 2). With reference to fig. 7, the dynamic threshold is evaluated mathematically using multiplicative model as,

$$\int_{\lambda_{Th}}^n f(x)dx = [1 - \beta](e^n - \lambda_{Th}) \tag{16}$$

and the same is computed using additive model as,

$$\int_{\lambda_{Th}}^n f(x)dx = [1 - \alpha](n - \lambda_{Th}) \tag{17}$$

where, n: Total number of sensor-cells in the system and x: Individual decision vector of the sensor-cells. Both of these two equations are powerful in the sense that on simplification, these culminate in transcendental equations for ' λ_{Th} ', which will finally produce two values for ' λ_{Th} ', one positive and the other negative. So, depending upon the nature of our application, we can select either '+ λ_{Th} ' or '- λ_{Th} '. The details of the computations for the above two equations are presented in *Appendix I*.

It may be noted that the formulation of the multiplicative model inherently leads to the inference for ' H_0 ', especially when the object-size is very small (i.e. 'k' is large). That means, there is always a natural tendency towards selecting ' H_0 ' *wrongly* and thereby committing a *Type II error*. Hence we need to consider the probability of Type II error, ' β ' in computing the required area (under hatch, refer fig. 7), and subsequently, ' λ_{Th} '. In contrast to this, the additive model suggests equally likely outcome, i.e. the model can select ' H_1 ', but may commit a *Type I error* by *rejecting* it too. That means, here we must consider the probability of Type I error, ' α ' in computing the desired area and the factor, (1- α) in eqn. 17 denotes the level of confidence we have in selecting the ' H_1 '.

However, choice of ' α ' or ' β ' will largely depend upon the value of ' n ', i.e. how large the sensor-cell system is or to that extent, how big is the sensor-matrix. Nevertheless, a *stricter* level (i.e. lower value of α or β) will lead to a tougher strategy for accepting the alternate hypothesis, viz. "signal is present". So, depending upon the exact use of the sensor system, ' α ' or ' β ' can be selected. For example, for a gross gripping of a comparatively large object we need not have a stricter confidence level and hence, even a probability of Type I error of 10% may be allowed in such a case. However, that won't be the right choice when the same sensory system is being used as a *stand-alone system* detecting *point-force*, instead of being augmented with the robot gripper. Hence, the user can take a final decision regarding the actual presence of object by analyzing $P(H_1)$, as obtained from the models.

Unlike the distinct value of the dynamic threshold as per the evaluation pattern proposed in fig. 7, the preferential selection model dictates the *dynamic threshold-band* (viz. $\lambda_{Th-mean}$ in fig. 5), as described earlier. It can be estimated using the statistical confidence level (α), i.e. probability of Type I error, as stated below. Here ' x ' & ' $f(x)$ ' represent individual decision-vector of the taxels and the exponential curve for $P(H_1)$, vide eqn. 14 respectively, while $[g(n)]_s$ signifies the maximum value of $U_G (\forall s=1,2,\dots,k)$.

$$\int_{\lambda_{Th-mean}}^{g(n)_s} f(x)dx = [1 - \alpha][g(n)_s - \lambda_{Th-mean}] \tag{18}$$

The planar area of the threshold-band, i.e. the *fuzzy-area* of *in-decision* can be computed as,

$$\int_{\lambda_{Th-initial}}^{\lambda_{Th-final}} f(x)dx = \int_{\lambda_{Th-initial}}^{g(n)_s} f(x)dx - \int_{\lambda_{Th-final}}^{g(n)_s} f(x)dx = [1 - \alpha][\lambda_{Th-final} - \lambda_{Th-initial}] \tag{19}$$

and the width of the threshold-band ($\delta\lambda_{Th}$) is defined as the numerical difference between $\lambda_{Th-final}$ and $\lambda_{Th-initial}$, i.e. ($\lambda_{Th-f} - \lambda_{Th-i}$) and modeled as,

$$\delta\lambda_{Th} = \frac{\alpha}{4} g(n) \quad (20)$$

However, choice of ' α ' will largely depend upon the value of ' $g(n)$ ', i.e. how intense is the effect of relative dependency in the sensor-matrix or to that extent, how large is (p,q) tuple. Nevertheless, a *stricter* level (i.e. lower value of α) will lead to a tougher strategy for accepting the alternate hypothesis, viz. "object is present".

2.2.3.5 Fusion optimization: advantage HEBTEM

HEBTEM, augmented with our fusion models, has been found advantageous over the traditional optimization techniques followed hitherto, namely, [a] Log-likelihood Ratio Test (LLR) and [b] Neyman-Pearson (N-P) Test. These techniques, though used vastly in situations concerning distributed data fusion problems, do possess inherent drawbacks. Both of these methods simply rely on the basic fact that both ' P_0 ' and ' P_1 ' are un-biased, i.e. in case of a new data fusion problem, such as the detection of the object-presence by the gripper sensor, both ' H_0 ' and ' H_1 ' are equally likely to occur. However, this pre-assumption of equally likeliness of the hypotheses is not valid for situations like robotic grasping and sensing the presence of object in the gripper-jaw. With regard to grasp analysis, there can be two domains of hypothesis metric, which has got *in-built biasing*, e.g. a] situations where either ' H_0 ' or ' H_1 ' is biased and b] situations where ' H_0 ' or ' H_1 ' are associated with penalty coefficients. In fact, neither LLR nor N-P test is fit for handling these two environments with impeding bias. We shall now investigate these situations in detail.

a. Situations where either ' H_0 ' or ' H_1 ' is biased

For an un-biased equally likely situation, the ratio between P_0 and P_1 is always 1.0, because the probabilities of both null and alternate hypotheses are 0.50. Mathematically it implies,

$$P_0 / P_1 = P(H_0) / P(H_1) = 1.0 \quad (21a)$$

and

$$\text{we denote, } \lambda_0 = P_0 / P_1 \quad (21b)$$

This ratio between P_0 and P_1 is being used to compute *global threshold* (λ_0) for the fusion problem, in general. As per equation (21b), the working formula for λ_0 will simply be the ratio between P_0 and P_1 in all *equally likely* cases, wherein the numerical value for the global threshold will be 1.0. However, since the numerical value of λ_0 is the deciding factor for both LLR and N-P tests, we need to judge the validity of the same under *biased situations*. For example, if for a typical case, H_0 is biased with a higher probability to occur due to some application-specific reason, the numerical value of λ_0 will not be equal to 1.0. For example, consider the situation, wherein the global threshold is computed as $\lambda_0 = P_0 / P_1 \equiv P(H_0) / P(H_1) = 0.7/0.3$, i.e. $\lambda_0 > 1.0$. Similarly, the value of λ_0 will be less than 1.0, in case a situation gets biased with H_1 . Thus, we surely need some other measurand for λ_0 that will be applicable for non-equally likely and/or biased hypothesis cases, as LLR and N-P are not suitable in such situations. The reason being in case of robotic gripping, we generally come across situations wherein only a 'point-object' or very small object is being grasped, leaving majority of the *taxels* free from getting excited. Hence, in such a situation, we need to bias the environment with the alternative hypothesis (H_1) in order to get fusion paradigms successfully. Likewise, biasing of hypothesis is a must for related situations, e.g. exciting the gripper sensor with a 'point-force'. Nonetheless, in situations wherein our main concern is

to disassociate the noise effects from the valid sensor data so that no erroneous reading can crop in during situations where no object is present physically, we need to bias the environment vis-à-vis optimization process with the null hypothesis (H_0).

b. *Situations where 'H₀' or 'H₁' are associated with penalty coefficients*

Here the general expression for *global threshold* (λ_0) is given as,

$$\lambda_0 = \frac{P(H_0)[C_{10} - C_{00}]}{P(H_1)[C_{01} - C_{11}]} \quad (22)$$

where, ' C_{ij} ' refers to the *cost* (penalty) of accepting ' H_i ' when ' H_j ' is true ($\forall i, j = 0, 1$). Now, for a non-specific case, it goes very fine if we assume the values of the cost-coefficients, viz. numerically C_{10} , C_{00} , C_{01} & C_{11} to be 1, 0, 1 & 0 respectively. As a matter of fact, these are the standard values of the cost-coefficients used in majority of the fusion problems and hence the numerical value of the global threshold becomes 1.0. However, the *impended bias* situation does arise not only because of the probabilistic values of the null and alternative hypotheses but also the cost involved in accepting the incorrect hypothesis. For example, if a specific situation demands inherent bias to be incorporated, then, λ_0 will be a function of both $P(H_k, \forall k = 0, 1)$ and $C_{ij} (\forall i, j = 0, 1)$. In other words, we can certainly have non-zero values for C_{00} & C_{11} and non-unity values for C_{10} & C_{01} . In a way, this metric of evaluating global threshold is not unique and cannot be tackled by LLR or N-P method, when all ' C_{ij} 's are numerically different. In case of robotic grasp, we often need to use one or more penalty coefficients, as the exact model for λ_0 should account for instances like detecting point-force, grasping micro-objects, rectifying the readings from faulty taxels or correcting noise-levels of the taxels. In such situations, we need to use eqn.22, wherein the value of λ_0 will not be equal to unity and thereby that value of λ_0 will be unfit for LLR or N-P to process further.

Thus, we can observe that both of the well-accepted optimization tests, namely, LLR and N-P, do possess hindrances while tackling fusion problem pertaining to robotic gripping and these tests fail to address the divergent situations, such as biased or non-equally likely hypotheses and penalty factors. And, it is apparent that we need to have suitable metric for global threshold, which will be *dynamic* and able to handle such *biased hypotheses*. As a matter of fact, fusion problem in such situations should ideally be considered with *on-line observation* values and *posteriori processing* using suitable model. In that respect, our model (HEBTEM) proves to be a viable option in processing on-line sensory data from the *taxels* using the metric of dynamic threshold (λ_{Th}). The developed method is capable of tackling the situation of *selective biasing*, as the method is solely based on experimental observations and not any a-priori assumption.

3. Spotlight on the matrix sensor and jaw-gripper used for case-studies

3.1 Matrix sensor: case-study I for additive & multiplicative models

The prototype version of the sensory system (external dimension: 175 mm. x 160 mm. x 20 mm), used in the case study, has been optimally designed for a moderately spaced layout to house three categories of sensor units, viz. resistive ('R'), capacitive ('C') and Piezo ('P') cells in a matrix layout. The "R-cells", spaced in 4x4 array, have been designed in the form of small slender 'struts', with a rectangular cross-section (5 mm. x 4 mm., with a 2 mm. diameter blind hole inside). A pair of strain gauges is pasted on the opposite walls of the struts. The capacitive cells, on the other hand, have been placed in a 5x5 matrix and these cells (15 mm. x

12 mm. x 5 mm.) have been designed taking into account the compliancy and overall sensitivity of the individual units, i.e. top & bottom plates and the dielectric layer. Figure 8 illustrates the schematic of the plan view of the of the matrix sensor used for the present study. A quasi-compliant protrusion pad atop protects these planar matrix-cells, having triangular / trapezoidal /spherical *serrations* embedded in it. Replaceable type pads are used, having triangular, trapezoidal or spherical serrations embedded. The protrusion pad has been designed in a way to make it quasi-compliant, shear stress-resistive and light-weighted. In the *assembled* version of the sensor system, a direct contact is being established between the struts and the serrations through slender pins, enabling the transmission of force(s) to the respective R-cells. Figure 9 schematically presents the internal disposition of the sensory assembly. 4 nos. PVDF sensors (P-cells, dimension: 25 mm. x 13 mm. x 205 μm) are mounted on the underneath of the protrusion (rubber) pad in a customized manner, so as to arrest micro-strains in both X & Y planes of the pad. The placement layout of the P-cells is illustrated in fig. 10.

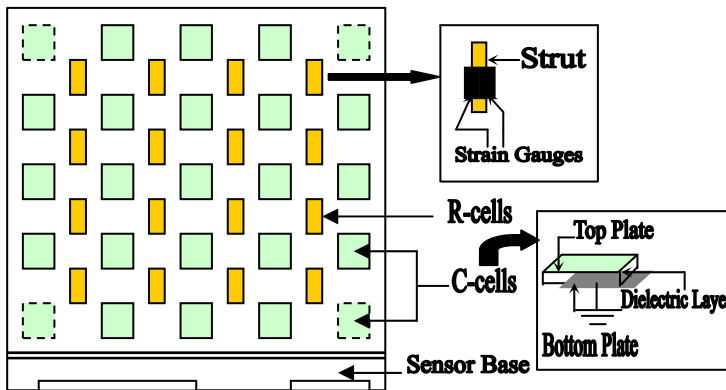
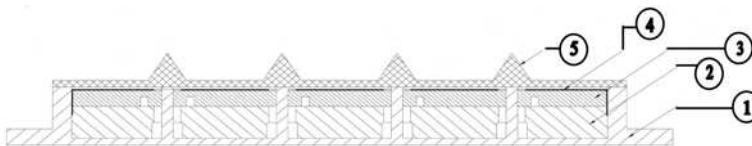


Fig. 8. Design metrics of the matrix sensor used in the case study I



Legends:

- 1: Base Plate
- 2: Bottom Support Plate [for the struts]
- 3: Top Guide Plate
- 4: Top Support Plate
- 5: Protrusion Pad

Fig. 9. Sectional view of the sensor assembly in case study I

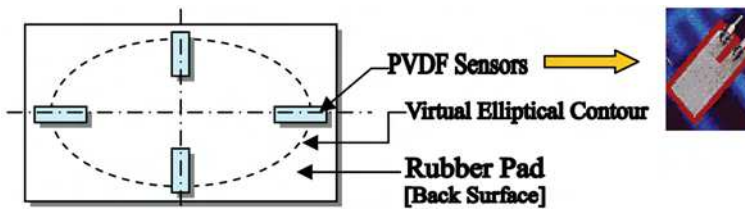


Fig. 10. Layout of the protrusion pad of the matrix sensor in case study I

The sensory system is being interfaced with a control circuitry, developed indigenously. The design is conceived as embedded system, with the provision for real-time processing of sensory signal. The control circuitry is conceptualized as optimally suited size, which necessarily compels minimum numbers of the measuring components for both R & C-cells. Sensory signals in analog form (mV) are being generated, as and when the cells are being *activated* through external force / *excitation*. The force-induced excitation gets manifested either in the form of *strains* generated in the strain gauges of the R-cells or by a change in capacitance in the C-cells, through the *instantaneous deformation* of the dielectric layer. The analog signals, so generated, are transferred to the control circuitry board (in the form of PCB) and are processed through stabilized circuits. The signals generated from the individual R & C-cells, then pass through micro-controller card and generate the final output signal. These *raw* output signals can be displayed over the VDUs (through serial communication with a PC or by using CRO) in real-time. The most appropriate fusion model is then superimposed on these raw data to get *unified* output.

3.2 Instrumented jaw gripper: case-study II for preferential selection model

The mechanical assembly of the planar parallel two-jaw robotic gripper, used in this case-study, comprises six major functional elements, namely, a] drive mechanism & associated drive train; b] motion transferring mechanism (through servomotor system); c] jaw assembly; d] drive for jaw movement; e] sensor assembly and related hardware and f] mounting structure (for assembling with the robot wrist). Nonetheless, the sensor system, augmented with the gripper body, includes the following four types, viz. a] *miniaturized load cell* for grip force evaluation [one per jaw, i.e. 2 in total]; b] *Infrared LED* for detection of object's presence /absence (three per jaw, i.e. 6 in total); c] *force sensor* for auxiliary measurement of grip-force (strain gauge, four in total, symmetrically placed over the moveable link) and d] *Thin-beam sensor* (TBS) for 'slip' measurement (five per jaw, i.e. 10 in total). Figure 11a presents a photographic view of the fabricated instrumented jaw gripper, with sensory interfaces (⊕) fitted inside the jaws, while the snapshots of the load cell (LC) & TBS (used for the slip sensor grid) are illustrated in fig. 11b,c respectively.

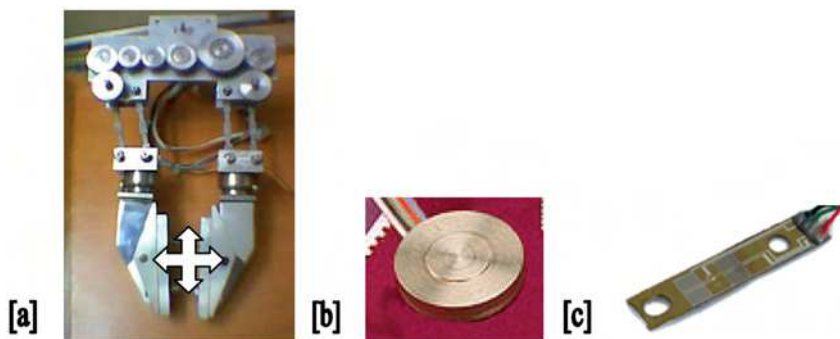


Fig. 11. Photographic view of [a] jaw gripper assembly [b] LC & [c] TBS used in case-study II
The fabricated hardware of the gripper system has suitable provision for easy mounting as a 'stand-alone' unit as well as while being interfaced with the wrist of the robotic manipulator. The drive system is through electrical d.c. servo-motor and the generated

Thank You for previewing this eBook

You can read the full version of this eBook in different formats:

- HTML (Free /Available to everyone)
- PDF / TXT (Available to V.I.P. members. Free Standard members can access up to 5 PDF/TXT eBooks per month each month)
- Epub & Mobipocket (Exclusive to V.I.P. members)

To download this full book, simply select the format you desire below

